MAGNETITE THERMAL ENERGY STORAGE FOR CSP PLANTS

Muhammad Sheik[1], Tshiamo Segakweng[2], and Karabelo Sekhuthe[3]

[1] CSIR, Meiring Naude Road, Brummeria, Pretoria, South Africa; Phone: 012 841 4132; Email: MSheik@csir.co.za

[2] CSIR; E-mail: TSegakweng@csir.co.za

[3] CSIR; E-mail: KSekhuthe@csir.co.za

Abstract: The Department of Mineral Resources and Energy estimates that the industrial sector is the largest consumer of energy in South Africa. Approximately 66% of energy end-use in industry is for heat generation during manufacturing. South African industry has been previously developed in the context of low energy prices for coal and electricity. This has resulted in a wide range of industrial processes that are inefficient and carbon intensive. With rising fuel prices, the prospect of fossil fuel depletion, and the continuous global effort to minimise environmental impact, it is necessary to develop alternate energy sources for heat generation. A significant portion of thermal energy can be generated using solar technology. However, solar energy supply is variable in nature and does not always match demand. It is therefore necessary to integrate thermal energy storage systems into solar plants to ensure availability. Thermal energy can be stored in three main ways namely, sensible, latent and thermochemical heat form. Magnetite is a material that undergoes an antiferromagnetic phase change at ~570 °C. This causes a reversible spike in the heat capacity of the material. This is highly advantageous for thermal energy storage applications and allows it to store more heat than other typical sensible storage media. Magnetite is widely available in South Africa and is often a waste product of other production processes. A lab-scale prototype was developed to analyse the thermal storage characteristics of magnetite in an open (non-pressurised) system with air as the working fluid. The magnetite was heated using a gas burner in a packed bed reactor and discharged using ambient air. Magnetite has the ability to store heat up to 1000 ºC which makes it suitable for CSP plants. The experimental results will be used to validate a CFD model to inform future CSP plant designs and for industrial process heating applications.

Keywords: Thermal Storage; Magnetite; Packed Bed Reactor

1. Introduction

With the world moving towards renewable energy, recent years have also seen advances in a range of storage technologies. It has been argued that because thermal energy storage (TES) has a combination of high power density and low energy costs making it an interesting option as a long-term storage technology. Thermal energy can be stored in three main ways namely; sensible, latent and thermochemical heat form. Sensible heat is the simplest method to store thermal energy and depends on the temperature change, mass of storage material and specific heat capacity of the material. TES technology is advancing, and it is imperative to use a low-cost thermal energy storage material (TESM), so as to stay economically relevant in a new growing field [1].

TES systems use electricity/heat to heat up a material. The heated material is then stored in an insulated container to store the energy until it is needed. The heat can be converted back to electricity through a power conversion device, or it can be used directly for process heating applications in industry.

One of the central issues associated with thermal energy storage is the development of a working body that has desirable properties (i.e., thermal conductivity, heat capacity, density, price, availability, and eco-friendliness). The main issue of a great number of current technologies is the excessive capital cost, which can prevent them from being successful in a market with no incentive schemes.

The International Energy Agency has drawn up categories that a thermal energy storage material is supposed to satisfy, the list is as follows [2]:

- Low commercial cost
- Acceptable eco-balance
- Stable up to 1000 °C
- Large thermal storage capacity (higher than 2.6 $MJ/m^3.K$)
- Available in industrial quantity
- Important lifetime (over 25 years)
- Compatibility with the HTF; and
- Easy implementation.

Magnetite is a common iron oxide (Fe_3O_4) mineral found in

rocks. It is the most commonly mined iron ore [3]. Magnetite is recognized as an inert compound that is almost entirely nontoxic to all living organisms [4], and its thermophysical properties have been researched and seem to be suitable and stable for TES applications.

Magnetite has been shown to have many advantages such as high availability, low cost, ecological friendliness, and non-flammability [1]. The one disadvantage of magnetite is its low thermal conductivity, and for this reason it has not been studied extensively for TES applications.

The most interesting characteristic of magnetite is the heat capacity which makes it an attractive material for TES. At approximately 570 °C it undergoes an antiferromagnetic phase transition which is reversible. This causes a spike in the heat capacity (refer to Figure 1) of the material. This is highly advantageous for thermal energy storage applications as heat is not only stored sensibly but also in latent form. Therefore, magnetite can store more heat than typical sensible heat storage materials such as rock and sand.

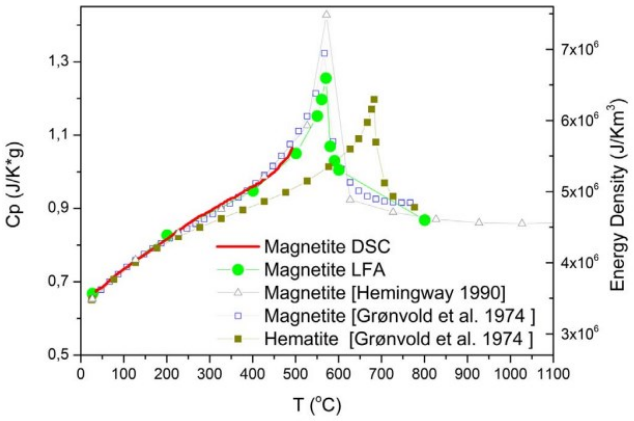

Figure 1. Heat capacity and energy density of magnetite [1]

Thermal energy storage is a crucial component of CSP systems, allowing them to generate electricity beyond daylight hours [5]. Excess thermal energy generated during sunny periods is stored as heat in various storage mediums with high heat retention properties. This stored thermal energy can then be used to continue producing steam and electricity during periods when the sun isn't shining, allowing them to provide reliable electricity output, thereby contributing to renewable energy generation with reduced intermittency. Magnetite has the ability to store heat up to 1000 ºC which makes it suitable for CSP plants [6]. Magnetite could be integrated into a thermal storage system of a CSP plant. During the charging phase, when the CSP plant is producing excess heat, the heat could be used to heat up the magnetite, storing thermal energy in the material. During the discharging phase, when electricity generation is required but there is no sunlight, the heat stored in the magnetite can be released to produce steam and drive turbines for electricity generation [7]. The system used in this investigation was regenerated at approximately 750 ºC (which is achievable by concentrated solar collectors) and the experimental results are presented and used to validate a CFD model.

There is limited research on the applications of magnetite for heat storage currently. The aim of this paper is to investigate the performance of magnetite for high-temperature thermal storage applications.

2. Experimental Apparatus

2.1. Test Rig

A packed bed thermal storage rig was developed at the Council for Scientific and Industrial Research (CSIR). The major components include a blower, LPG burner and packed bed reactor. The setup is shown in Figure 2.

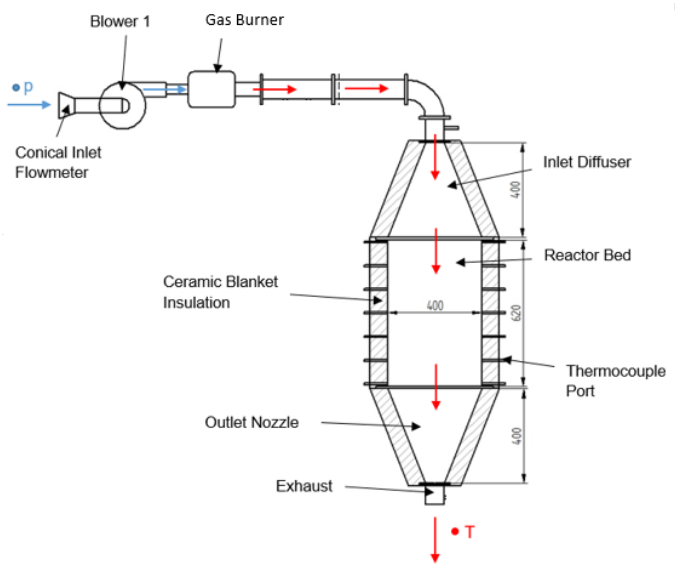

Figure 2. Diagram of packed bed test rig

For the charging cycle, the blower draws in air from the environment, through the conical inlet flow meter. The pressure differential at the throat of the conical inlet is measured to determine the mass flow through the rig. The air is then heated by the gas heater where the temperature is increased to ~750 ºC. The arrows in Figure 2, represent the flow path of the air moving through the system. Blue is representative of ambient air while red is representative of hot air. The hot air, exiting the burner, is supplied to the packed bed reactor.

The cylindrical packed bed reactor has a diameter of 400 mm and a height of 620 mm which constitutes an active volume of approximately 78 litres. A diffuser is attached to the inlet of the packed bed to distribute the air more evenly. A nozzle is attached to the exit of the packed bed to allow a smoother flow of air through

the rig. To minimise heat losses to the environment, the reactor wall is insulated with a ceramic fibre blanket of 75 mm thickness.

2.2. Temperature Sensor locations

The reactor comprises of several thermocouple ports to determine the temperature profiles through the packed bed. The thermocouples were positioned at 100 mm increments (refer to Figure 3) along the axis of the reactor.

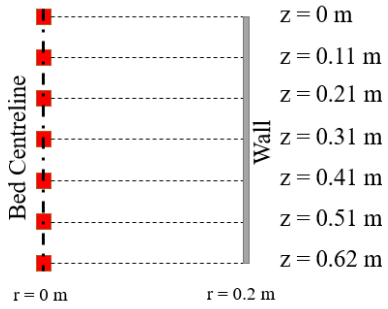

Figure 3. Thermocouple locations in packed bed reactor

2.3. Magnetite Samples

Approximately two hundred kilograms of Fine grade Magnetite (80-86% passing 45 μm) was purchased from a local supplier with a magnetite content of ≥95% and a density of >4500 kg/m^3. The powder was then compacted, at 'CERadvance Engineering Ceramics' to form 20x20 mm cylinders (refer to Figure 4) to allow for packing into a reactor for testing. The cylinders were randomly packed into the reactor.

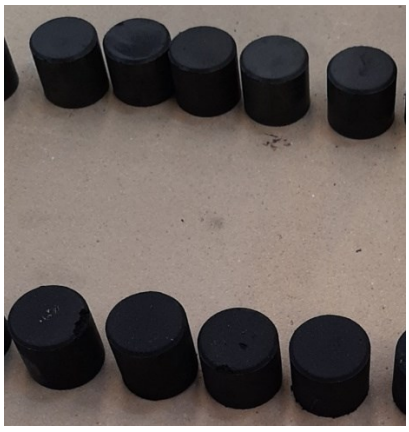

Figure 4. Magnetite samples at CERadvance

3. Experimental Results

The magnetite was heated from the top of the packed bed reactor and left to stand, for approximately 15 minutes, during which the flow direction was reversed. Ambient air was then supplied to the reactor until the heat was completely discharged. The primary type of thermal storage is sensible heat storage which is a direct form of heat storage and is a function of the temperature, heat capacity of the storage medium, and the mass of the storage medium. However, at a temperature of approximately 570 ºC, a phase change occurs in magnetite which causes a spike in the heat capacity of the magnetite. This is referred to as an antiferromagnetic change which allows additional heat (latent heat) to be stored in the medium.

3.1. Temperature

The temperature profiles achieved during testing are presented in Figure 5. The air temperatures were measured using K-type thermocouples, which were calibrated by 'Repair and Metrology Service (Pty) Ltd,' with a maximum deviation of 0.2 ºC. In region 1 (between t=0 h and t=1.75 h), the temperature of the air, entering the reactor (z=0 m), was ramped up to 750 ºC using a gas burner. The temperature was transferred from the upper layers to the lower layers as depicted by the thermocline moving through the packed bed. The burner and blower were shut off (at t=1.75 h) when the outlet temperature approached 250 ºC. This was due to a temperature limitation on the thermal plastic exhaust hose. However, at this point in time, at least half the reactor (z=0.3m) was heated to above 600 ºC which is beyond the antiferromagnetic phase change which occurs at ~570 ºC. This would have enabled the magnetite to store some latent heat in addition to the sensible heat stored. Between t = 1.75 h and t=2 h (region 2) the bed was left to stand, to change the system configuration, to reverse of the flow direction for discharging the heat stored. In region 3 (t=2 h to t=5 h) ambient air (at approximately 20 ºC) was supplied until the entire packed bed was cooled.

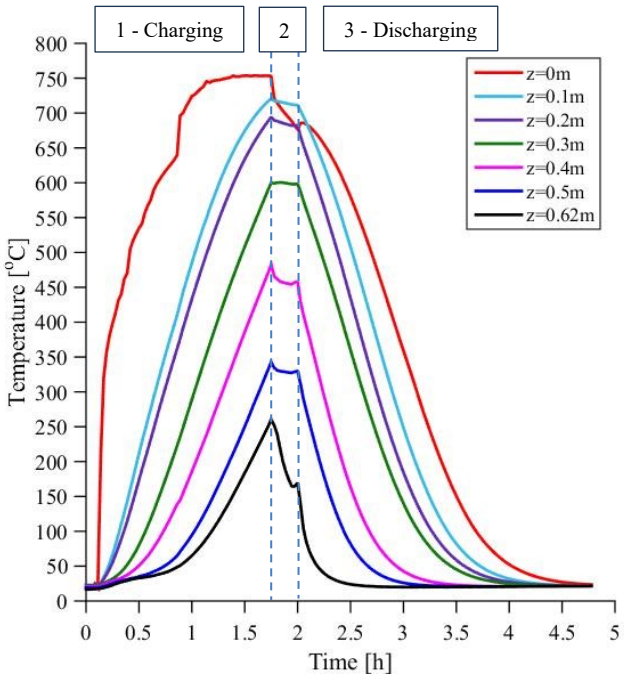

Figure 5. Temperature profiles

3.2. Mass flow rate

The mass flow rate results are presented in Figure 6. Between t=0 and t=1h the gas flame was not consistent which caused the air flow rate to fluctuate. The blower speed was carefully controlled to ensure that the temperature achieved was adequate for heating up the magnetite. As the temperature was ramped up the flow rate did stabilise at approximately 96 kg/h for the charging cycle. In region 2 the blower was switched off and therefore the flow rate was 0 kg/h. For the discharging cycle, since there were no limitations on flow rate it was increased to 115 kg/h.

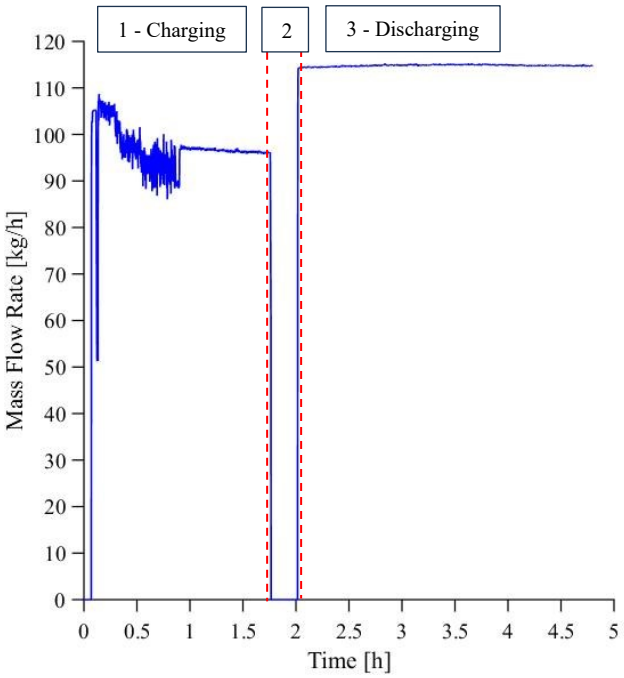

Figure 6. Mass flow rate

3.3. Heat Stored and Discharged

The amount of energy stored and released is presented in Figure 7. This was calculated from the product of the mass flow rate, specific heat capacity and temperature difference between the inlet and outlet of the reactor. By integrating the curves shown (in MATLAB) it was calculated that 25.05 kWh was absorbed by the magnetite during charging and 22.55 kWh was released from the reactor during discharging. This equates to an overall efficiency on 90%. This can be improved by increasing the thickness of the insulation surrounding the reactor.

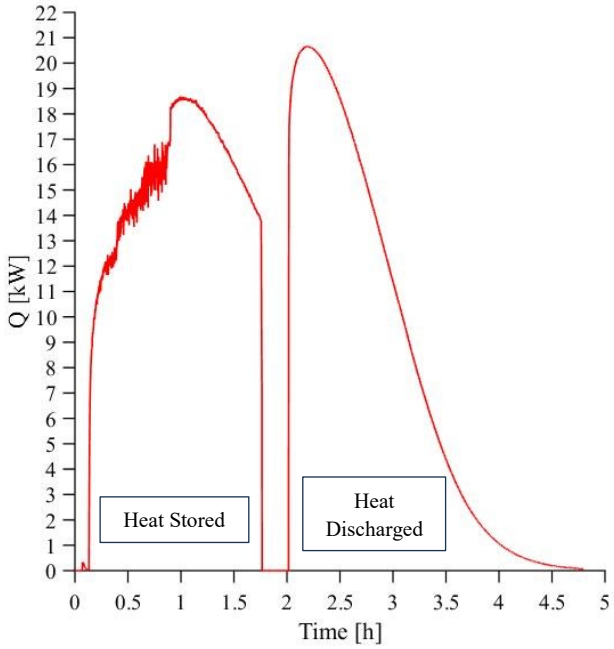

Figure 7. Heat stored and discharged

4. CFD Model

A CFD model was set up in FloEFD to model the heat storage in magnetite. The steps taken to set up the model are described in the next sections.

4.1. Solid Materials

- Packed bed walls and inlet and outlet cones: Inconel (selected from database)
- Insulation: Ceramic Fibre Blanket (User defined)

4.2. Assumptions

- Density of Magnetite powder: 4500 kg/m^3
- Void fraction: 0.5 (Calculated based on magnetite mass, density and reactor volume)
- The packed bed can be modelled as a porous medium

4.3. Steps taken to define porous medium

4.3.1. Pressure Drop

The Eisfeld and Schnitzlein equation was used to determine the pressure drop through the packed bed, with respect to flow rate, and can be calculated from equation 1 [8]. This equation is based on experimental data and accounts for particle shape, effect of Reynolds number on coefficients and wall effects. The results agree with the widely used Ergun equation [9] for lower mass flow rates (between 0 and 0.035 kg/s) as shown in Figure 8.

$$\frac{\Delta P}{Z\rho_f {U_z}^2} \mathrm{D} \frac{\varepsilon^3}{(1-\varepsilon)} = \frac{190{A_w}^2}{Re_{Erg}} + \frac{A_w}{B_w} \quad (1)$$

Where:

$$Re_{Erg} = \frac{\rho_f U_z D}{\mu_f (1-\varepsilon)} \quad (2)$$

$$A_w = 1 + \frac{2}{3(D_r/D)(1-\varepsilon)} \quad (3)$$

$$B_w = [2(D_r/D)^2 + 0.77]^2 \quad (4)$$

$$D = \frac{6\sum V_p}{\sum A_p} \quad (5)$$

Z: Height of packed bed (m)

ΔP: Pressure drop through packed bed (Pa)

U_z: Superficial fluid velocity (m/s)

ε: Bed void factor

ρ_f: Density of fluid flowing through packed bed (kg/m^3)

μ_f: Viscosity of fluid flowing through packed bed (Pa.s)

D: Particle size (m)

D_r: Diameter of reactor (m)

V_p: Particle volume (m^3)

A_p: Particle surface area (m^2)

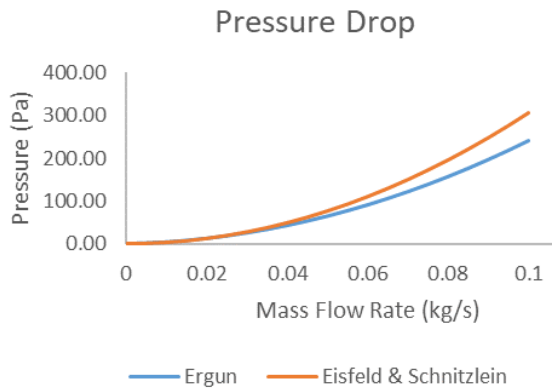

Figure 8. Pressure drop vs mass flow rate

4.4. Boundary Conditions

4.4.1.Charging

- Inlet (top): Experimental inlet temperature and mass flow rate
- Outlet (bottom): Ambient pressure

4.4.2. Discharging

- Inlet (bottom): Ambient temperature (~20 ºC) air at flow rate of ~0.032 kg/s
- Outlet (top): Ambient pressure

4.5. Running the model

During the charging cycle, approximately half the packed bed was heated to at least 600 ºC which took 1.75 h. The bed was left standing for 0.25 h as was done in during experimental testing. The discharging cycle was run thereafter by supplying air at approximately 20 ºC, until the entire packed bed cooled to ambient, which also took approximately 2.5 h. The temperature distribution through the packed bed is shown in Figure 9 at a time of 1.75 h.

4.6. Validation of model against experimental data

The experimental results and the CFD temperature profiles are plotted on the same set of axes in Figure 10. There is a good correlation between the two. Figure 11 shows the energy stored and discharged for CFD Model and experimental testing on the same plot. The results agree within 5% which is generally acceptable in literature [10]. The deviation could be due to the fact that the magnetite was mixed with approximately 5 wt% binder, before compacting, which could have affected the thermal properties and density slightly. The reactor also contains several thermocouple ports which could have led to leaks and heat losses, although great care was taken during testing to ensure that the ports were sealed.

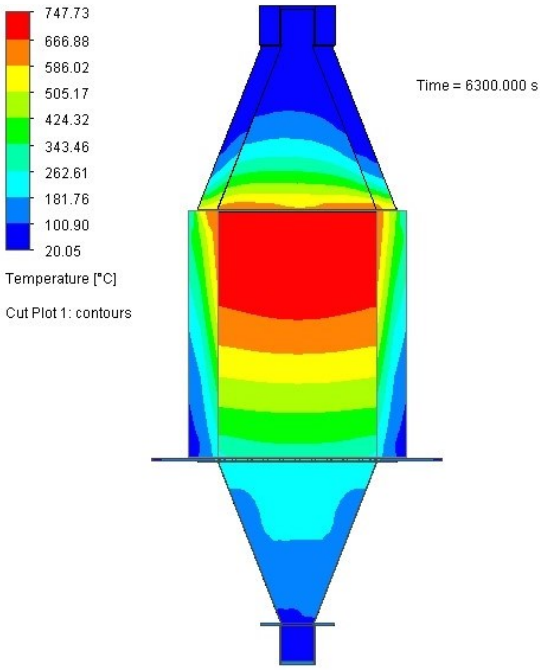

Figure 9. Magnetite packed bed CFD model

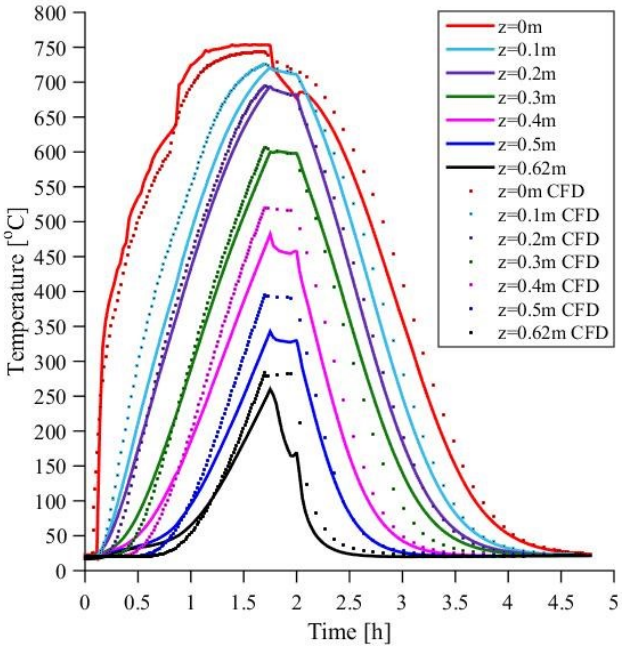

Figure 10. Experimental and CFD temperature profiles

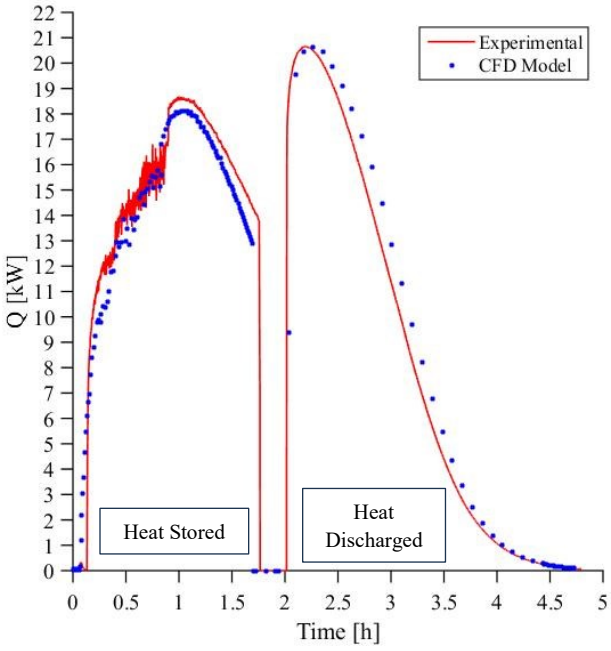

Figure 11. Energy stored and discharged in experimental and CFD model

5. Conclusion

Magnetite is a promising material for thermal storage and has the ability to store heat up to 1000 ºC, which makes it suitable for CSP plants and industrial regenerators. A lab-scale prototype was setup to investigate the performance of magnetite for high-temperature thermal storage applications. Since the antiferromagnetic phase change occurs at ~570 °C, the magnetite in the upper half of the reactor was heated to above 600 ºC. The entire packed bed could not be heated due to temperature limitations on the exhaust of the reactor. After heating the magnetite, ambient air was supplied to discharge the heat stored. From the experimental results, it was calculated that 25.05 kWh was absorbed by the magnetite during charging. This equates to an energy storage density of 320 kWh/m^3. During discharging 22.55 kWh was released from the reactor which results in an overall efficiency of 90% which is higher than a typical sensible heat storage system of 70% [11]. A CFD model was developed to inform future CSP plant designs and for industrial waste heat recovery applications. The experimental results were used to successfully validate the CFD model.

References

[1] Y. Grosu, A. Faik, I. Ortega-Fernández and B. D'Aguanno, "Natural Magnetite for thermal energy storage: Excellent thermophysical properties, reversible latent heat transition and controlled thermal conductivity," *Solar Energy Materials & Solar Cells,* no. 161, pp. 170-176, 2017.

[2] Y. F. Baba, H. Ajdad, A. . A. Mers, Y. Grosu and A. Faik, "Multilevel comparison between magnetite and quartzite as thermocline energy storage materials," *Applied Thermal Engineering,* vol. 149, pp. 1142-1153, 2019.

[3] H. M. King, "Magnetite and Lodestone," Geology News and Information, [Online]. Available: https://geology.com/minerals/magnetite.shtml. [Accessed June 2022].

[4] B. Kalska-Szostko, U. Wykowska, D. Satula and P. Nordblad, "Thermal treatment of magnetite nanoparticles," *Beilstein Journal of Nanotechnology,* vol. 6, pp. 1385-1396, 2015.

[5] M. Mehos and H. Price, "Concentrating Solar Power Best Practices Study," June 2020. [Online]. Available: https://www.nrel.gov/docs/fy20osti/75763.pdf. [Accessed 14 August 2023].

[6] H. Qiu, W. Y, H. Chen, R. Wang, J. Yu and Y. Lin, "Influence of SiC on the thermal energy transfer and storage characteristics of microwave-absorbing concrete containing magnetite and/or carbonyl iron powder," *Construction and Building Materials,* vol. 366, no. 0950-0618, p. p.130191, 2023.

[7] U.S. Department of Energy, "Concentrating Solar-Thermal Power Basics," Solar Energy Technologies Office, [Online]. Available: https://www.energy.gov/eere/solar/concentrating-solar-thermal-power-basics. [Accessed 14 August 2023].

[8] K. G. Allen, T. W. von Backström and D. G. Kröger, "Packed bed pressure drop dependence on particle shape, size distribution, packing arrangement and roughness," *Powder Technology,* vol. 246, pp. 590-600, 2013.

[9] D. Thornhill, "Flow Through Packed Beds," University of Washington, [Online]. Available: https://faculty.washington.edu/finlayso/Fluidized_Bed/FBR_Fluid_Mech/packed_beds_fbr.htm. [Accessed 14 August 2023].

[10] "What is the suitable and acceptable error variations between the CFD results and experimental data?," ResearchGate, [Online]. Available: https://www.researchgate.net/post/What-is-the-suitable-and-acceptable-error-variations-between-the-CFD-results-and-experimental-data. [Accessed 26 September 2023].

[11] A. H. Abedin and M. A. Rosen, "Closed and open thermochemical energy storage: Energy- and exergy-based comparisons," *Energy,* vol. 41, pp. 83-92, 2012.